Supporting Information

Introduction of Cationic Charge into DNA Near the Major Groove Edge of a Guanine•Cytosine Base Pair: Characterization of Oligodeoxynucleotides Substituted with 7-Aminomethyl-7-Deaza-2'-Deoxyguanosine

Manjori Ganguly,[†] Ruo-Wen Wang,[†] Luis A. Marky[‡] and Barry Gold*[,†,]

[†]University of Pittsburgh, Department of Pharmaceutical Sciences, 3501 Terrace St., Pittsburgh, PA 15261 and [‡]University of Nebraska Medical Center, Department of Pharmaceutical Sciences, Omaha, NE 68198-6025

Table of Contents

Supporting Materials……S2

Supporting Methods……S2-S4

UV Spectroscopy……...S2-S3

Differential Scanning Calorimetry……..S3-S4

Circular Dichroism……...S4

Supporting Tables……S5

Supporting Figures……..S6-S17

Supporting References……S18

Materials and Methods:

Materials

All oligodeoxynucleotides were synthesized in the Department of Chemistry, Centre in Molecular Toxicology, Vanderbilt University, Vanderbilt, TN. The phosphoramidite derivatives of 7-(aminomethyl-7-deazaguanine (**1**) and 7-hydroxymethyl-7-deazagaunine (**2**) were prepared as previously described.[1] Phosphoramidite of 7-deazaguanine (**c^{7}G**) was obtained commercially (Glen Research). For the on-column oxidation of the phosphite to phosphate (1S)-(+)-(10-camphorsulfonyl) oxaziridine rather than I_2 was used for the incorporation of **c^{7}G** (Glen Research, Sterling, VA). The modified oligomers were purified using reversed-phase HPLC (Phenomenex, Phenyl-Hexyl, 5 μm, 250 mm × 10.0 mm) equilibrated with 0.1 M triethyl ammonium acetate (pH 7.0), desalted on a G-25 Sephadex column, and lyophilized to dryness. The samples were characterized by MALDI-TOF-MS. The dry oligomers were then dissolved in the appropriate buffer.

The oligodeoxynucleotide concentrations were determined using an extinction coefficient of 1.11 × 10^5 M^{-1} cm^{-1} (dodecamers) and 1.05 × 10^5 M^{-1} cm^{-1} (hairpins) at 260 nm and 25 °C assuming similar extinction coefficients for **1**, **2**, **c^{7}G**, and G.[2,3]

UV-Spectroscopy

Absorption versus temperature profiles (UV melts) for each duplex were measured at either 260 nm and/or 275 nm using a thermoelectrically controlled Varian Cary 300 spectrophotometer, interfaced to a PC computer for data acquisition and analysis. The temperature was scanned at heating rates of 1.00 °C/min. Melting curves as a function of strand concentration, 4–70 μM, were obtained to check for the molecularity of each molecule. Additional melting curves were obtained as a function of salt and osmolyte concentration to determine the differential binding of counterions and water molecules that accompanies their helix coil transitions.

UV melts were measured in the salt range of 16−216 mM NaCl at pH 7, and at a constant total strand concentration of 7 μM, to determine the differential binding of counterions, Δn_{Na^+}, which accompanied their helix−coil melting. This linking number was measured experimentally with the assumption that counterion binding to the helical and coil states of each oligonucleotide took place with a similar type of binding using the relationship:

$$\Delta n_{Na^+} = 0.483[\Delta H_{cal}/RT_M^2](\partial T_M/\partial \log [Na^+]).^{4,5}$$

The numerical factor corresponded to the conversion of ionic activities into concentrations. The first term in parentheses, $(\Delta H_{cal}/RT_M^2)$, was a constant determined directly from DSC experiments, where R was the gas constant. The second term in parenthesis was determined from UV experiments from the dependencies of T_M on salt concentration.

For the determination of Δn_w, UV melts were measured in the ethylene glycol concentration range of 0.5- 3.0 m at pH 7 and 10 mM NaCl and at a constant total strand concentration of 7 μM. The osmolalities of the solutions were obtained with a Wescor Vapro vapor pressure osmometer, Model 5520 (Logan, UT). These osmolalities were then converted into water activities, a_w, using the following equation:

$$\ln a_w = -(Osm/M_w);^{6}$$

where Osm is the solution osmolality and M_w is the molality of pure H_2O, equal to 55.5 mol/kg H_2O. Differential binding of water, Δn_w, was calculated using the relationship:

$$\Delta n_w = 0.434[\Delta H_{cal}/RT_M^2](\partial T_M/\partial \log a_W).^{4,5}$$

The $\Delta H_{cal}/RT_M^2$ term used in the determination of Δn_w at higher salt concentration is the one obtained experimentally at the particular salt concentration.

Differential Scanning Calorimetry

Heat capacities versus temperature profiles were measured with a VP-DSC differential scanning calorimeter (Microcal, Inc., Northampton, MA). The dry oligodeoxynucleotides were dissolved in 10 mM sodium phosphate buffer (pH 7) and adjusted to the desired ionic strength with NaCl for all unfolding experiments. The heat capacity profile for each DNA solution was measured against a buffer solution. In a typical experiment the reaction and the reference cells were each filled with 0.75 ml of solution. Temperature was scanned from 0 to 100°C at a rate of 0.75°C/min. The experimental curve was normalized

by the heating rate, and a buffer versus buffer scan was subtracted and normalized for the number of moles. The resulting curves were then analyzed with Origin version 7.0 (Microcal); their integration ($\int \Delta C_p \, dT$) yielded the molar unfolding enthalpy (ΔH_{cal}), which was independent of the nature of the transition.[7,8] The molar entropy (ΔS_{cal}) was obtained similarly, using $\int (\Delta C_p/T) \, dT$. The free energy change at any temperature T was then obtained with the Gibbs equation: $\Delta G°(T) = \Delta H_{cal} - T\Delta S_{cal}$.

Circular Dichroism

Circular dichroism (CD) measurements were conducted on a Jasco (model J-815) CD spectrometer (Easton, MD, USA). The spectrum of each duplex was obtained using a strain-free 1 cm quartz cell at low temperatures to ensure 100% duplex formation. Typically, 1 OD of a duplex sample was dissolved in 1 ml of a buffer containing 10 mM sodium phosphate (pH 7.0). The reported spectra correspond to an average of three scans from 220 to 350 nm at a wavelength step of 1 nm.

Table S1: Standard thermodynamic parameters for the formation of DNA complexes at 20°C[a].

OL	sequence	NaCl (mM)	T_M (°C)	ΔG^o (kcal/ mol)	ΔH^o (kcal/ mol)	$T\Delta S^o$ (kcal/ mol)	Δn_{Na+} (mol-1 DNA)	Δn_w (mol-1 DNA)	$\Delta\Delta G$ vs OL-1
1	5′-GAGAGCGCTCTC	10 100	48.7 66.1	-6.9 -12.5	-78.2 -92.0	-71.3 -79.5	-3.35 ± 0.17 -3.61 ± 0.18	-41 ± 3 -43 ± 4	-
10	5′-GA-**c^{7}G**-AGCGCTCTC	10 100	47.2 63.5	-6.1 -9.2	-72.0 -71.0	-65.9 -61.8	-2.46 ± 0.12 -2.30 ± 0.12	-31 ± 3 -28 ± 3	0.8 3.3
11	5′-GA-**1**-AGCGCTCTC	10 100	54.4 68.1	-7.9 -12.7	-75.5 -90.2	-67.6 -77.5	-2.43 ± 0.12 -2.68 ± 0.12	-26 ± 2 -29 ± 2	-1.0 -0.2
12	5′-GA-**2**-AGCGCTCTC	10 100	47.5 64.7	-3.3 -7.5	-37.9 -56.5	-34.6 -49.0	-1.45 ± 0.14 -1.83± 0.14	-8 ± 1 -10 ± 1	3.6 5.0

[a]All parameters are measured from UV (T_M) and DSC melting curves in 10 mM sodium phosphate buffer (pH 7.0). The observed standard deviations are: T_M (± 0.7), ΔH_{cal} (± 3%), $\Delta G°_{20}$ (± 5%), $T\Delta S_{cal}$ (± 3%).

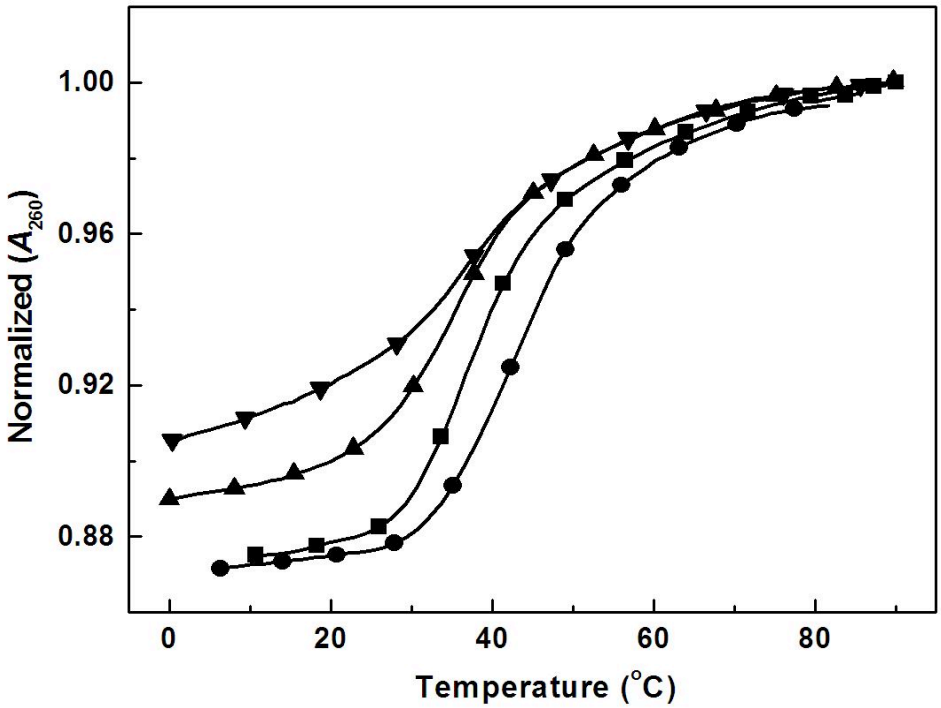

Figure S1: UV melting curves in 10 mM sodium phosphate buffer (pH 7.0), ~ 7 μM total strand concentration for OL-1 (■), OL-2 (▲), OL-3 (●) and OL-4 (▼)

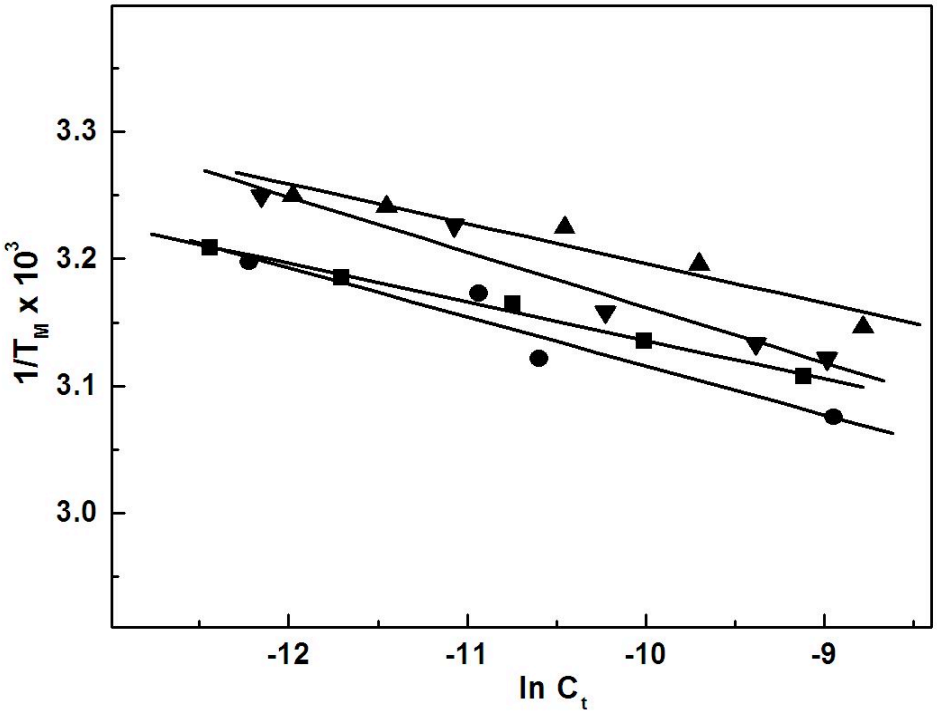

Figure S2: T_M dependence on strand concentrations in 10 mM sodium phosphate buffer (pH 7.0), 4-150 μM strand concentration at 260 nm for OL-1 (■), OL-2 (▲), OL-3 (●) and OL-4 (▼).

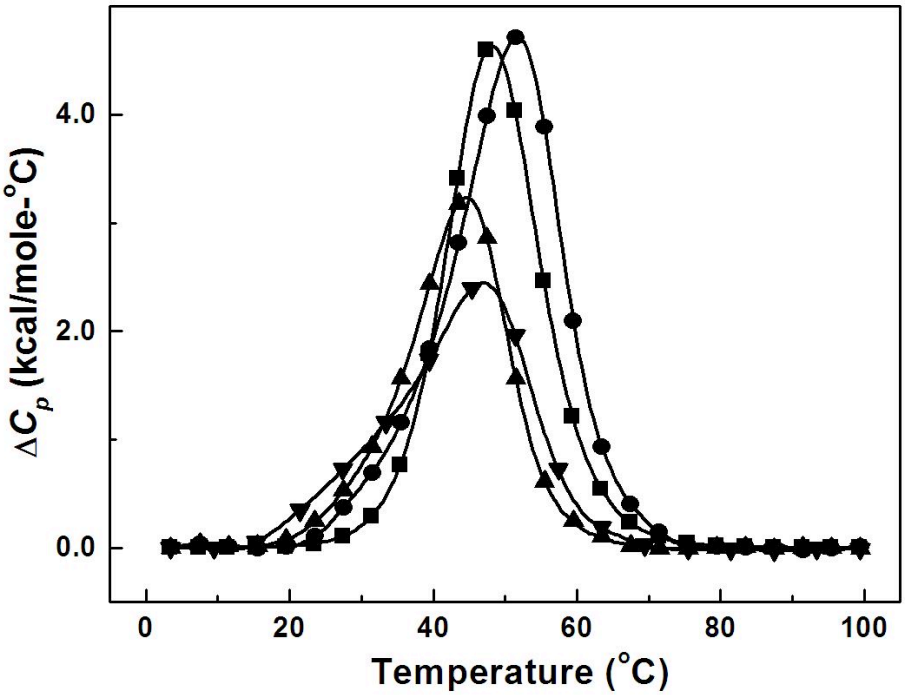

Figure S3: DSC curves in 10 mM sodium phosphate buffer (pH 7.0) for OL-1 (■), OL-2 (▲), OL-3 (●) and OL-4 (▼).

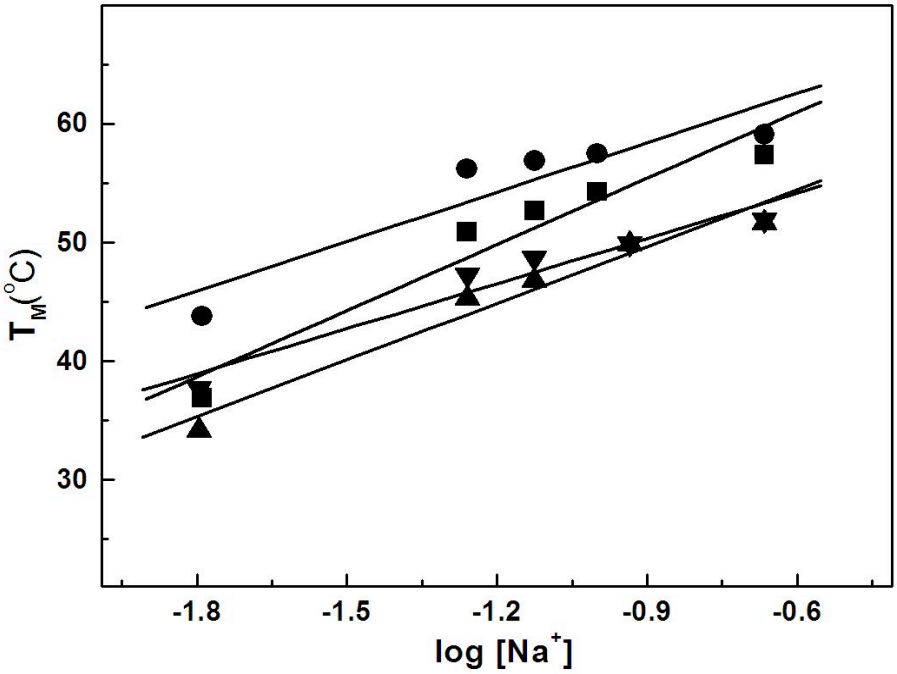

Figure S4: Dependence of T_M on sodium concentration for OL-1 (■), OL-2 (▲), OL-3 (●) and OL-4 (▼). The UV melting curves were obtained in 10 mM sodium phosphate buffer (pH 7.0) at a strand concentration of ~ 7 μM.

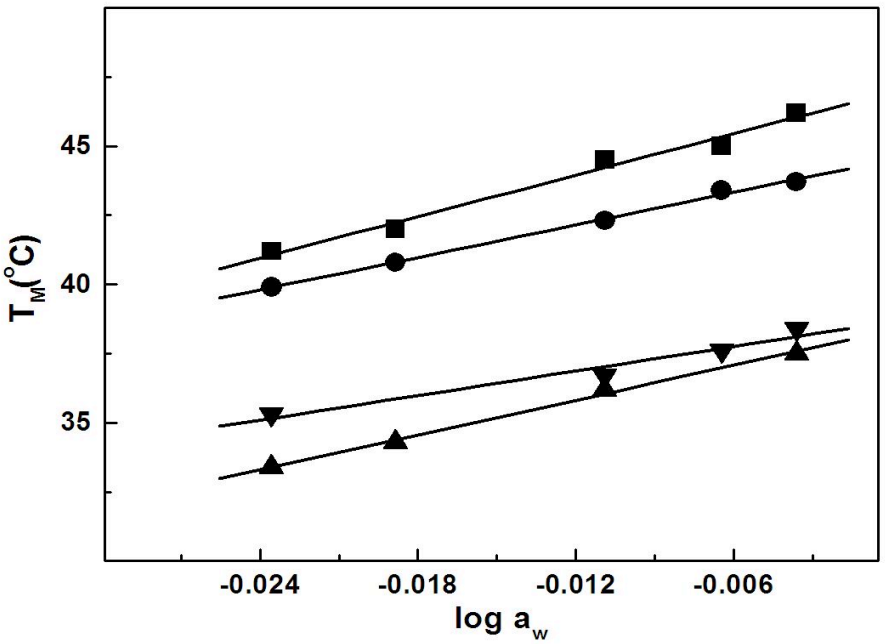

Figure S5: Dependence of T_M on osmolyte concentration for OL-1 (■), OL-2 (▲), OL-3 (●) and OL-4 (▼). The UV melting curves were obtained in 10 mM sodium phosphate buffer (pH 7.0) at a strand concentration of ~ 7 μM.

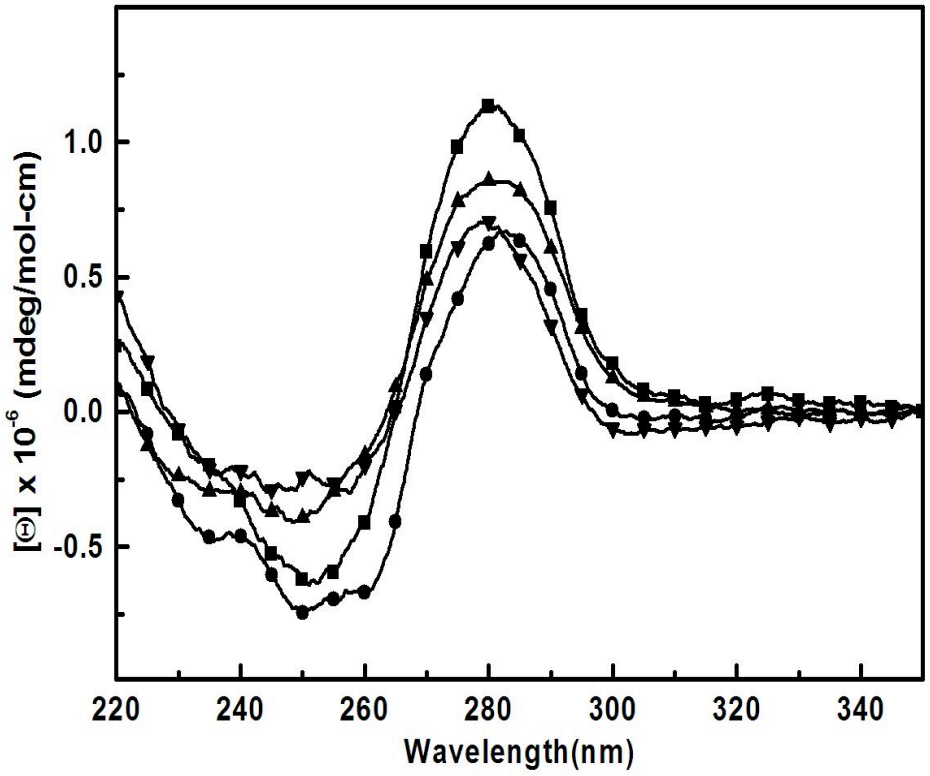

Figure S6: Differential CD spectra in 10 mM sodium phosphate buffer (pH 7.0), ~ 10 μM strand concentration for OL-1 (■), OL-2 (▲), OL-3 (●) and OL-4 (▼)

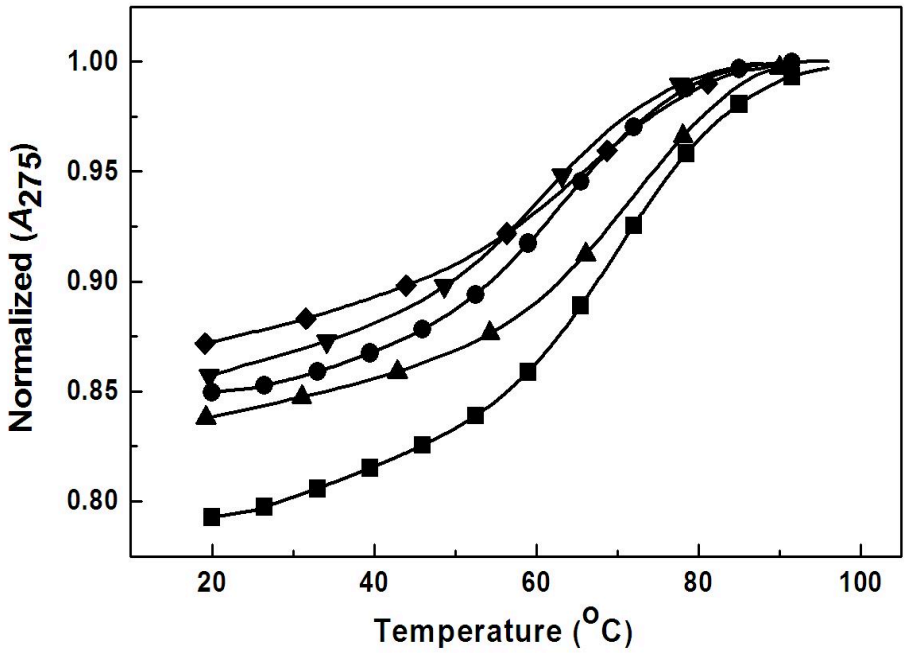

Figure S7: UV melting curves in 10 mM sodium phosphate buffer (pH 7.0), ~ 7 μM total strand concentration for OL-5 (■), OL-6 (●), OL-7 (▼), OL-8 (▲) and OL-9(◆).

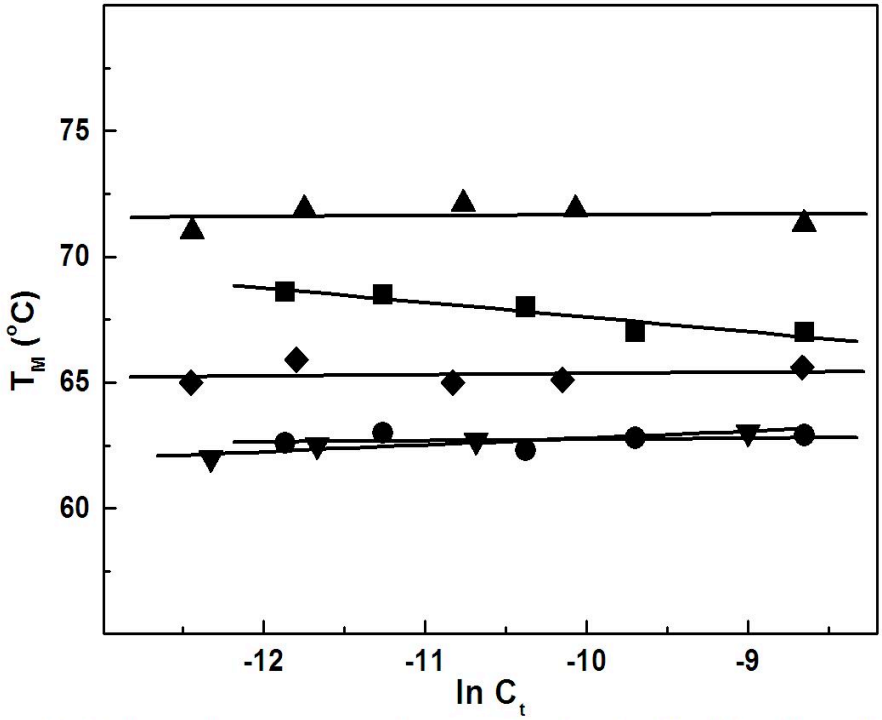

Figure S8: T_M dependence on strand concentrations in 10 mM sodium phosphate buffer (pH 7.0), 4-200 μM strand concentration for OL-5 (■), OL-6 (●), OL-7 (▼), OL-8 (▲) and OL-9(◆).

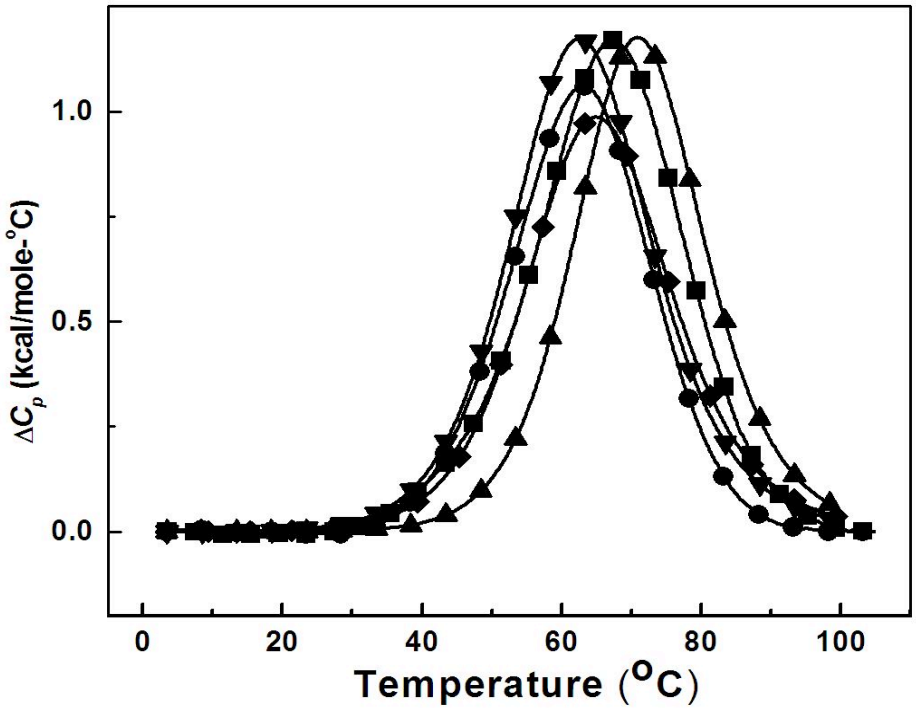

Figure S9: DSC curves in 10 mM sodium phosphate buffer (pH 7.0) for OL-5 (■), OL-6 (●), OL-7 (▼),OL-8 (▲) and OL-9(◆).

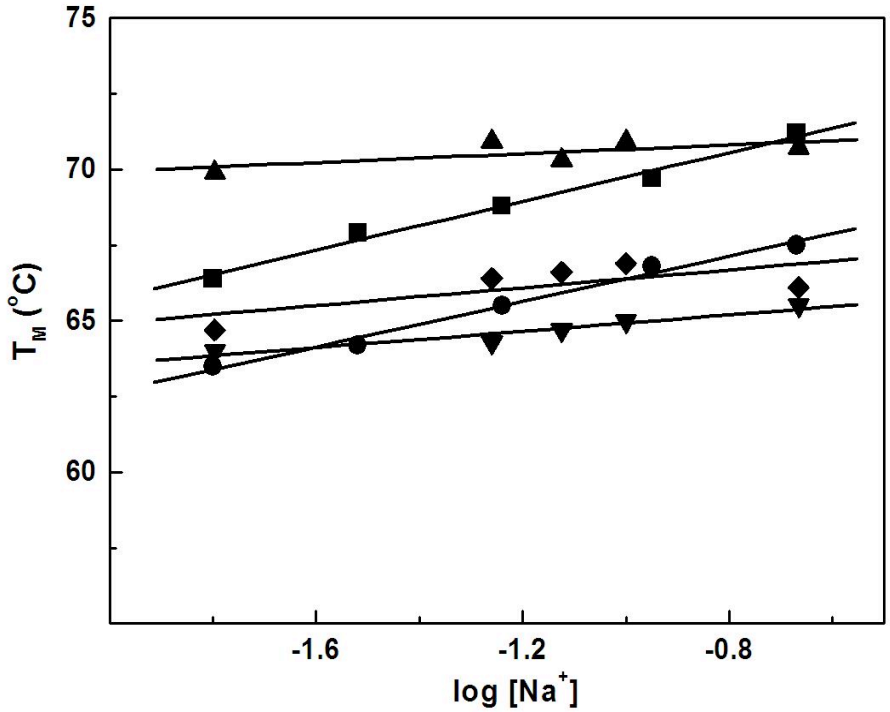

Figure S10: Dependence of T_M on sodium concentration for OL-5 (■), OL-6 (●), OL-7 (▼), OL-8 (▲) and OL-9(◆). The UV melting curves were obtained in 10 mM sodium phosphate buffer (pH 7.0) at a strand concentration of ~ 7 μM.

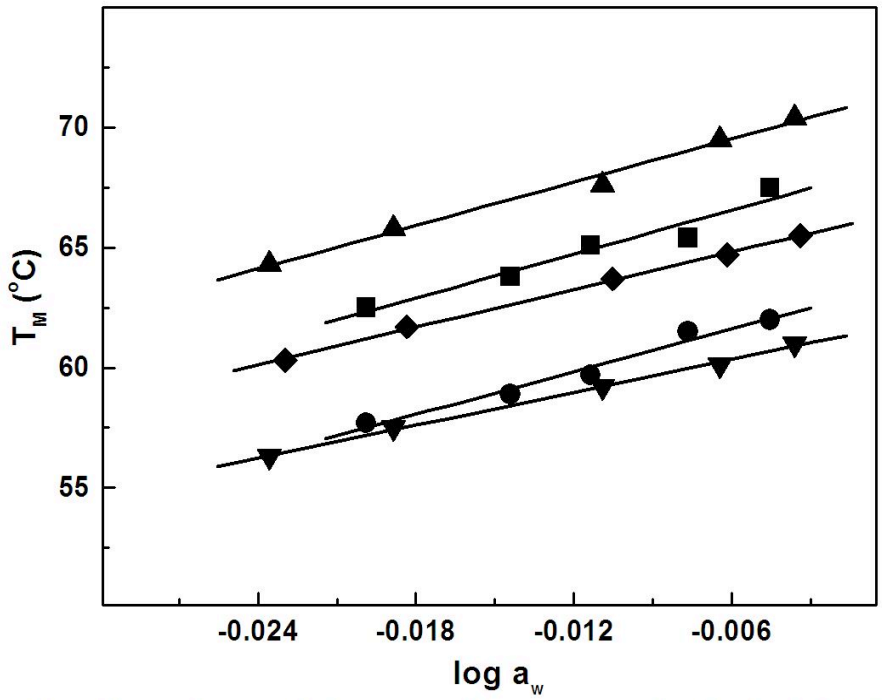

Figure S11: Dependence of T_M on osmolyte concentration for OL-5 (■), OL-6 (●), OL-7 (▼), OL-8 (▲) and OL-9(◆). The UV melting curves were obtained in 10 mM sodium phosphate buffer (pH 7.0) at a strand concentration of ~ 7 μM.

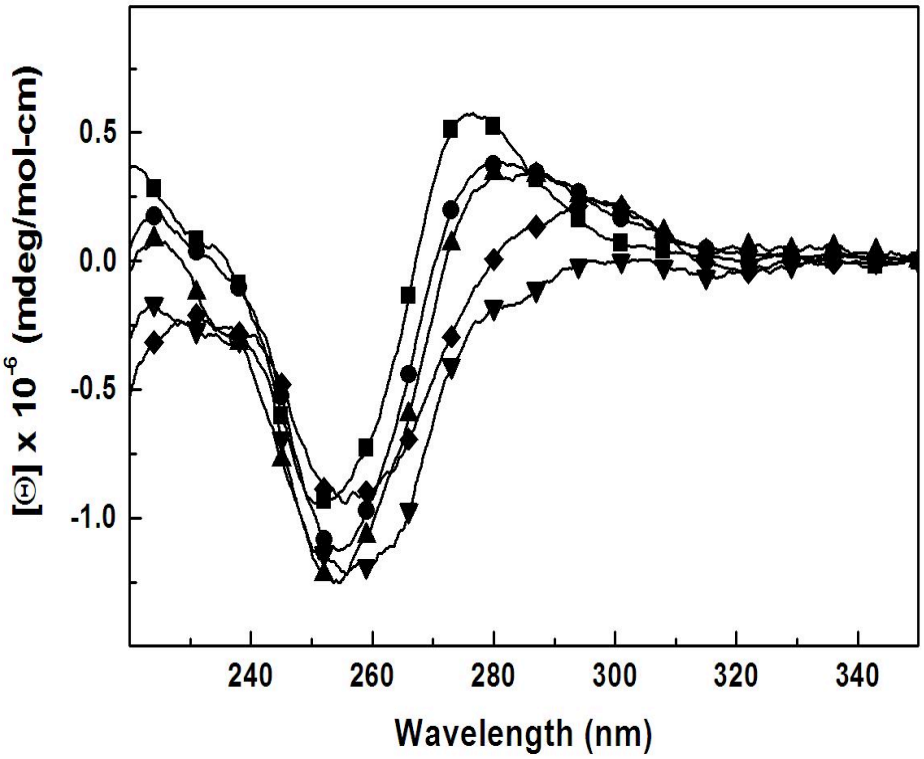

Figure S12: Differential CD spectra in 10 mM sodium phosphate buffer (pH 7.0), ~ 10 μM strand concentration for OL-5 (■), OL-6 (●), OL-7 (▼), OL-8 (▲)and OL-9(◆).

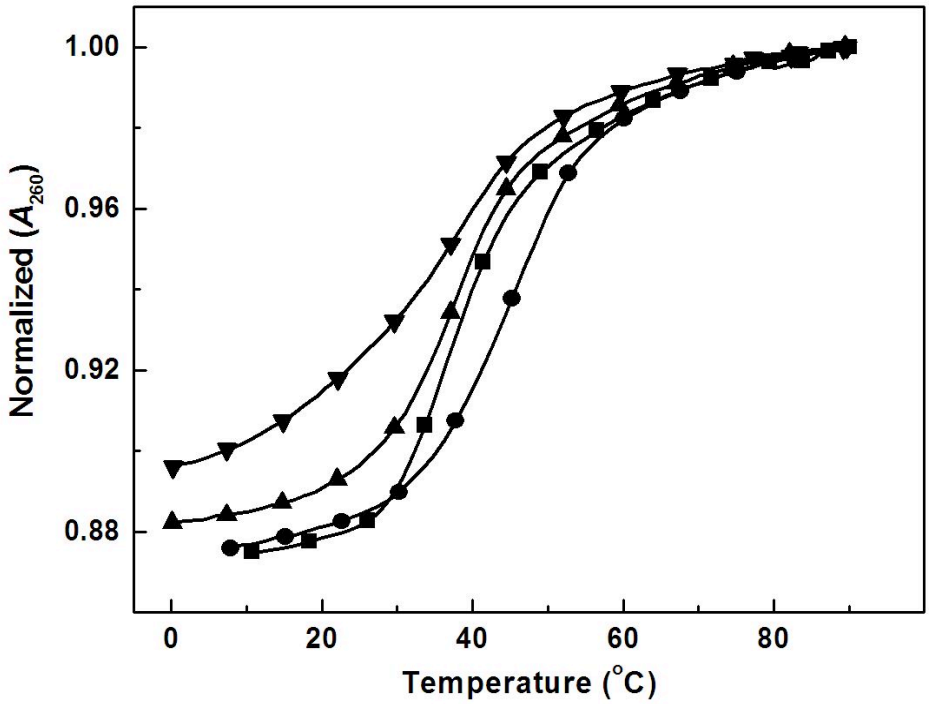

Figure S13: UV melting curves in 10 mM sodium phosphate buffer (pH 7.0), ~ 7 μM total strand concentration for OL-1(■), OL-10 (▲), OL-11 (●) and OL-12 (▼).

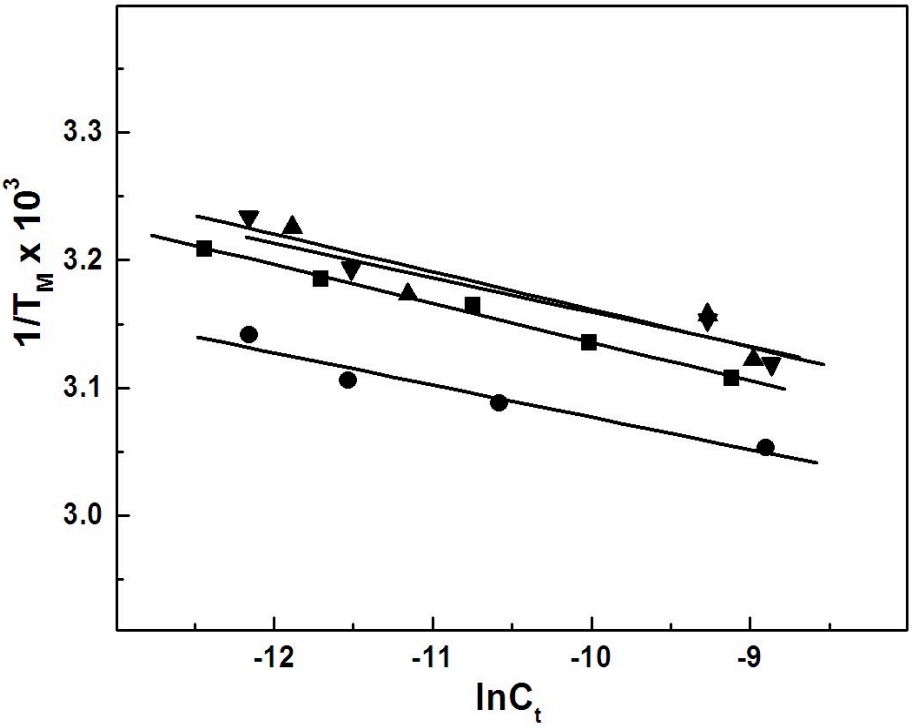

Figure S14: T_M dependence on strand concentrations in 10 mM sodium phosphate buffer (pH 7.0), 4-150 μM strand concentration for OL-1 (■), OL-10 (▲), OL-11 (●) and OL-12 (▼).

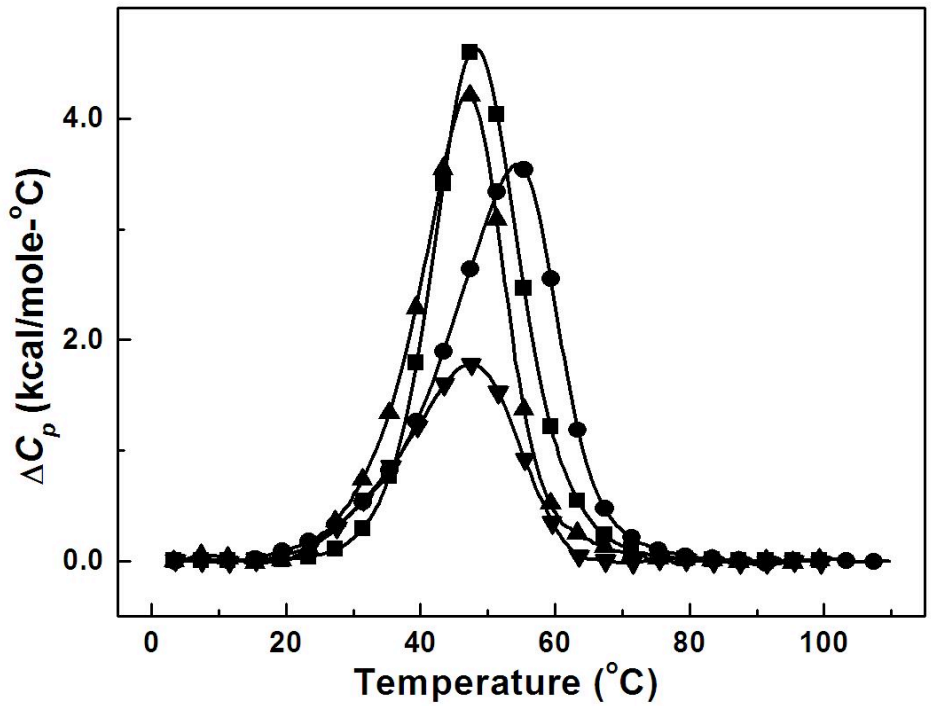

Figure S15: DSC curves in 10 mM sodium phosphate buffer (pH 7.0) for OL-1 (■), OL-10 (▲), OL-11(●), OL-12 (▼)

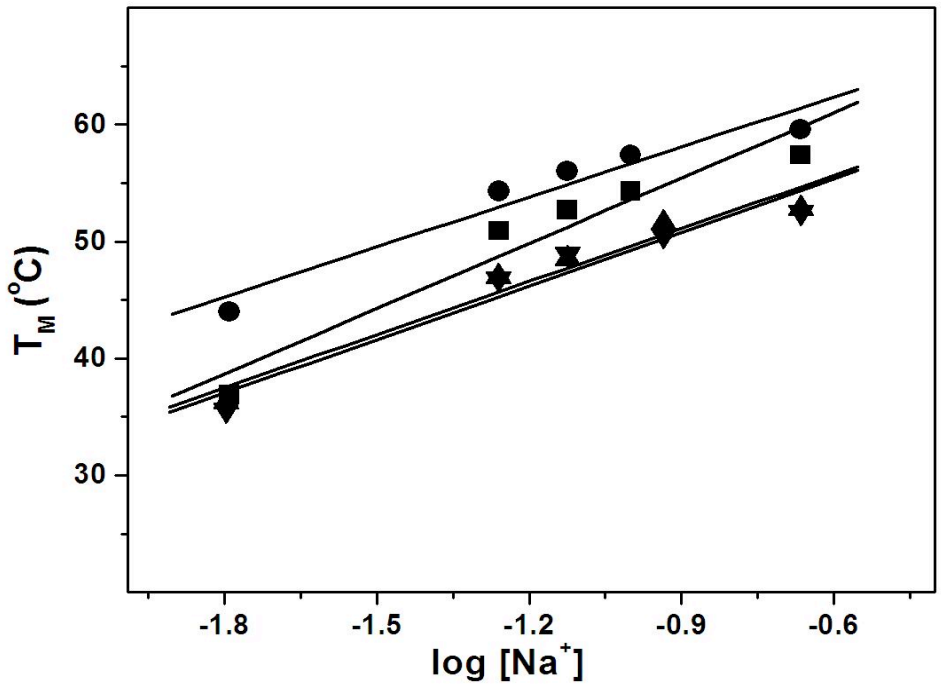

Figure S16: Dependence of T_M on sodium concentration for OL-1 (■), OL-10 (▲), OL-11 (●), OL-12 (▼). The UV melting curves were obtained in 10 mM sodium phosphate buffer (pH 7.0) at a strand concentration of ~ 7 μM.

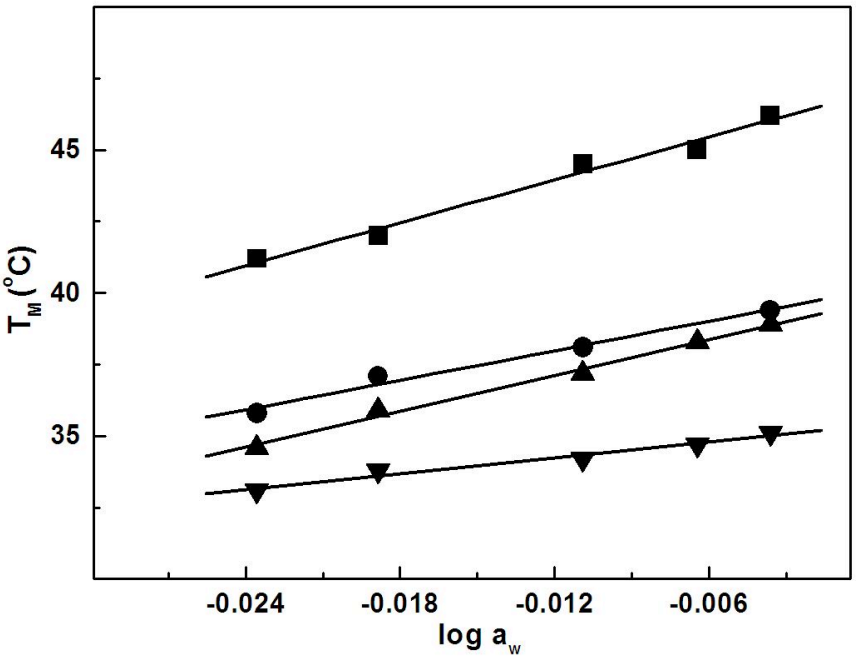

Figure S17: Dependence of T_M on osmolyte concentration for OL-1 (■), OL-10 (▲), OL-11 (●), OL-12 (▼). The UV melting curves were obtained in 10 mM sodium phosphate buffer (pH 7.0) at a strand concentration of ~ 7 μM.

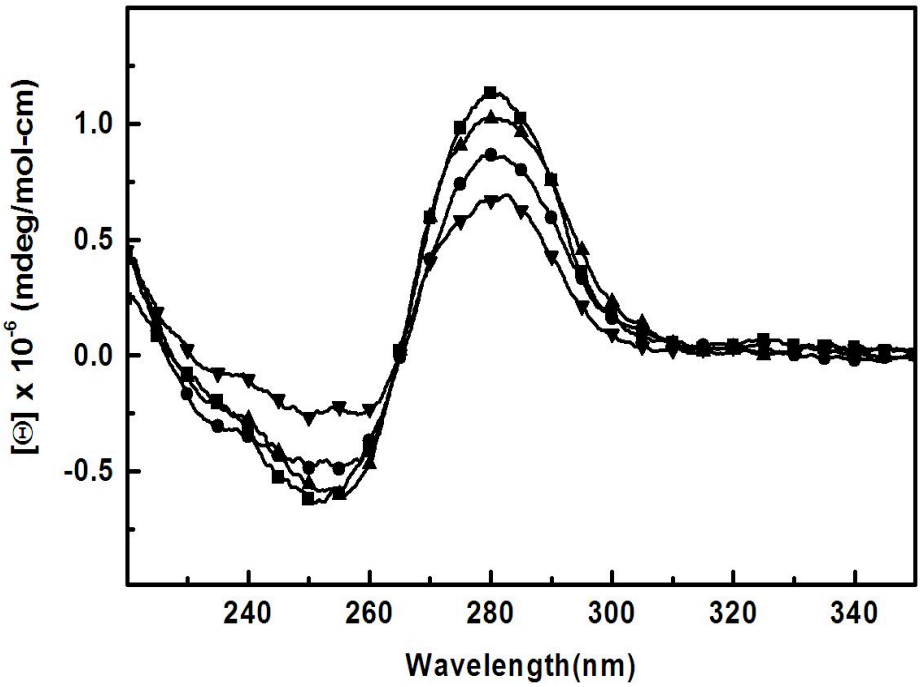

Figure S18: Differential CD spectra in 10 mM sodium phosphate buffer (pH 7.0), ~ 10 μM strand concentration for OL-1 (■), OL-10 (▲), OL-11 (●) and OL-12 (▼).

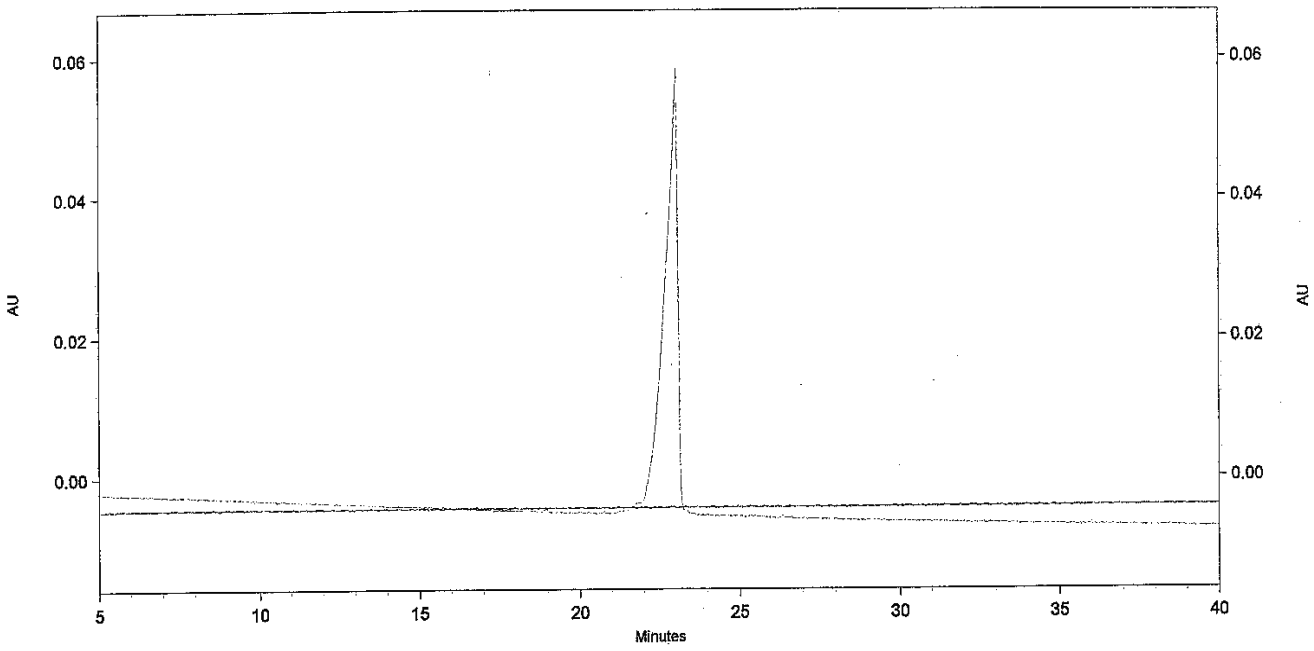

Figure S19: Capillary Electrophoresis data for the purification of **OL-3**.

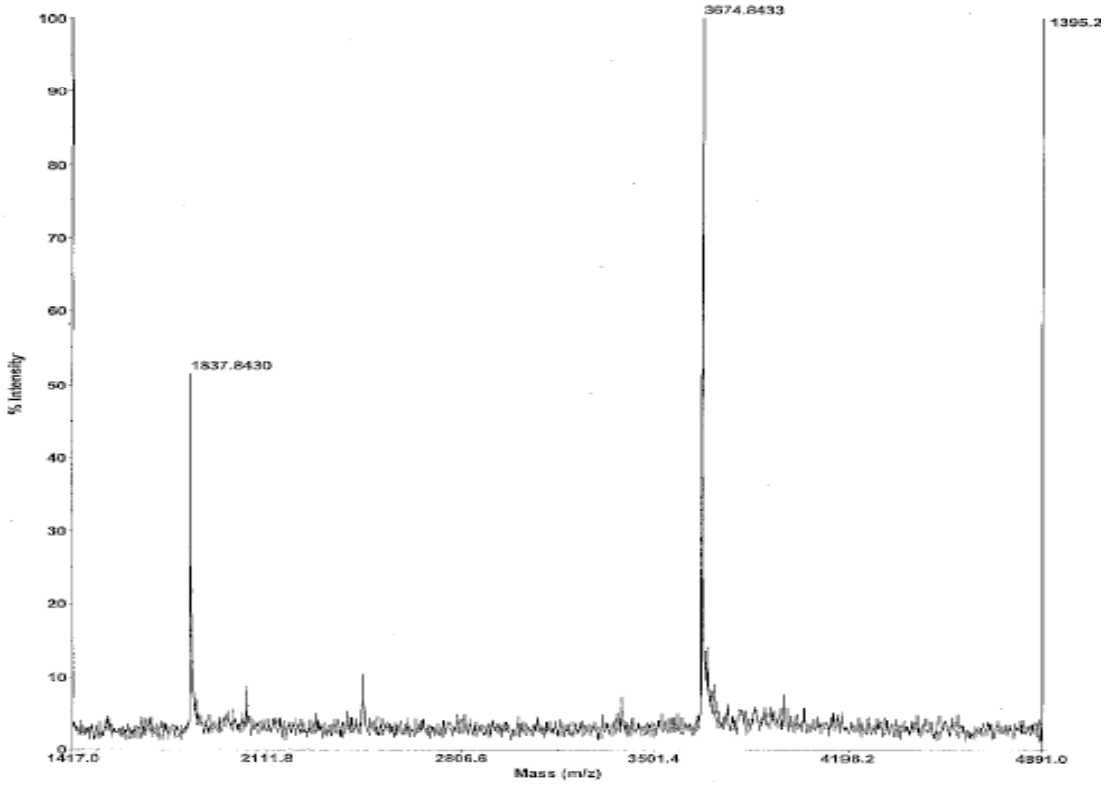

Figure S20: MALDI data for **OL-3**.

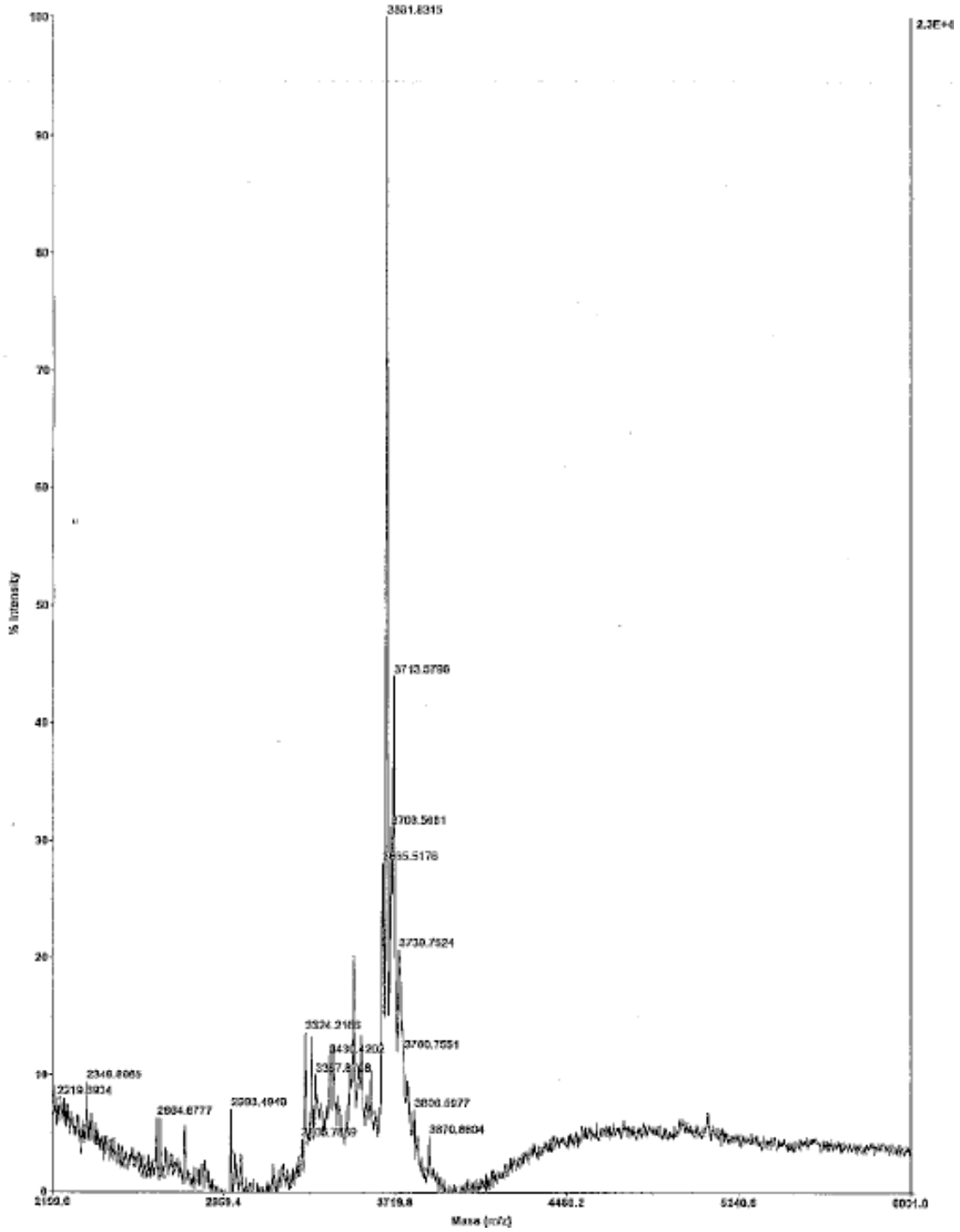

Figure S21: MALDI data for **OL-4**.

Relaxed stereoview to show the closest possible distance between the tethered amino groups in:

(a) **OL-1** (8.28 Å)

5'-G-A-G-A-**1**-A-G-C-T-C-T-C
3'-C-T-C-T-C-T-C-**1**-A-G-A-G

(b) **OL-** (4.00 Å)

5'-C-G-C-**1**-
3'-G-C-**1**-C-


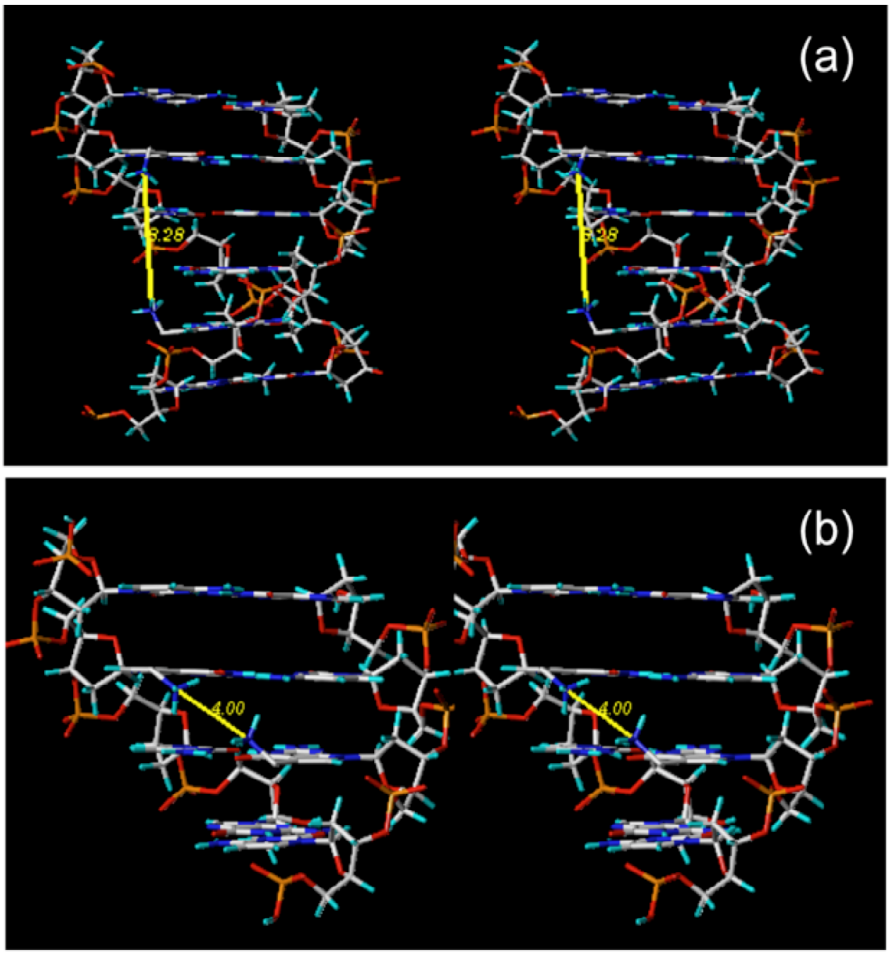

Figure S22:

References

(1) Wang, R.W.; Gold, B. *Org. Lett*., **2009**, 11, 2465-2468.

(2) Cantor, C. R., Warshow, M. M. and Shapiro, H. *Biopolymers* **1970**, 9, 1059-1077.

(3) Marky, L. A., Blumenfeld, K. S., Kozlowski, S. and Breslauer, K. J. *Biopolymers* **1983**, 22, 1247-1257.

(4) Cantor, C.R.; Schimmel, P.R. *Biophysical Chemistry* **1980**, W.H. Freeman and Company: New York.

(5) Kaushik, M., Suehl, N. and Marky, L. A. *Biophysical Chemistry* **2007**, 126, 154-164

(6) Courtenay, E. S., Capp, M. W. Anderson, C. F. and Record, M. T. J. *Biochemistry* **2000**, 39, 4455-4471.

(7) Marky, L. A. and Breslauer, K. J. *Biopolymers* **1987**, 26, 1601-1620.,

(8) Rentzeperis, D., Marky, L. A., Dwyer, T. J., Geierstanger, B. H., Pelton, J. G. and Wemmer, D. E. *Biochemistry* **1995**, 34, 2937-2945.